Structure and Properties of Poly(2,5-di-*n*-dodecyl-1,4-phenylene) Depending on Chain Length

T. F. McCarthy, H. Witteler, T. Pakula, and G. Wegner*

Max Planck Institut für Polymerforschung, Postfach 3148, D-55021 Mainz, Germany

Received September 8, 1994; Revised Manuscript Received September 5, 1995[⊗]

ABSTRACT: An investigation of the morphologies of solution-cast/melt-pressed films of poly(2,5-di-*n*-dodecyl-1,4-phenylene) by X-ray diffraction revealed a sandwich type structure, with layers of aliphatic side chains perpendicular to the substrate surface separating layers of main chains extended parallel to the substrate surface. The physical properties were highly influenced by the local conformational mobility of the side chains. With increasing temperature, the concentration of gauche conformations in the side chains increases strongly over a temperature range from −50 to 190 °C and was reflected in a large negative coefficient of thermal expansion for the direction normal to the main chain layers, $\alpha_a = -9.72 \times 10^{-4}$/K. The linear decrease in the layer spacing of the side chains can be correlated to the linear temperature dependence of the tensile properties of solution cast films (E, $\sigma_b \approx T^{-1}$). The M_w dependence of LC phase formation was investigated by DSC, polarizing microscopy, and rheological measurements. In the molten phase, polymers of $M_w < 30\,000$ showed only an isotropic phase, polymers of $44\,000 \leq M_w \leq 73\,000$ gave coexisting isotropic/anisotropic phases, and polymers having $M_w \leq 94\,000$ showed only a single anisotropic phase. Polymers that formed anisotropic melts behaved as shear thinning non-Newtonian fluids, and the zero-shear viscosity scaled as $\eta_0 \sim M_w^{3.2}$. The viscosity of polymers that formed isotropic melts was independent of deformation frequency, and a scaling law $\eta_0 \sim M_w^{2.9}$ seems to hold.

Introduction

Poly(*p*-phenylene) belongs to a class of rigid-rod polymers that are distinguished by their stiff main chains, the repeat units of which are capable of only a single rotation around their chain axis. Such polymers include poly(*p*-phenylene-2,6-benzodiimide), poly(*p*-phenylene-2,6-benzodithiazole), and, due to restricted rotation of the amide linkage, poly(*p*-phenyleneterephthalamide),[1] each of which is recognized as having exceptional mechanical properties. Poly(*p*-phenylene) would be expected to show mechanical properties consistent with those of other members of this class of polymers, as well as exceptional thermal, oxidative, and electrical properties. The development of poly(*p*-phenylene), however, has been hindered by various synthetic obstacles. Unlike other rigid-rod polymers that have been successfully prepared by condensation methods, poly(*p*-phenylene) contains only carbon−carbon linkages. Attempts to synthesize poly(*p*-phenylene) have included the direct oxidation of benzene using copper catalysts, coupling reactions involving transition metal catalysts, and indirect methods that utilize a precursor polymer to obtain poly(*p*-phenylene) in a final step.[2−15] The synthesis is further complicated by the polymer's lack of solubility, such that oligomeric materials are obtained due to premature precipitation.

An important step in the successful synthesis of functionalized poly(*p*-phenylene)s was the development of a palladium-catalyzed coupling reaction of an aryl bromide with an arylboronic acid.[16] By adopting this method to polymer synthesis, a series of functionalized poly(*p*-phenylene)s with pendant alkyl groups has recently been reported by Wegner et al.[17−19] The palladium-catalyzed coupling reaction has also been extended to the synthesis of water-soluble poly(*p*-phenylene)s containing pendent carboxylic acid groups by Novak et al. A modification of the Pd(0) cross-coupling reaction was employed, in that bis(1,3-propanediol)ester derivatives of diboronic acids were coupled with aryl halides.[20−23]

One objective of the present investigation was to synthesize poly(2,5-di-*n*-dodecyl-1,4-phenylene)s having a sufficiently high degree of polymerizations, such that initial information about the mechanical properties of these types of polymeric materials could be obtained. Poly(*p*-phenylene)s having long pendant groups were chosen to obtain a good balance of physical properties. The desired physical properties included polymers sufficiently rigid that they could be readily oriented, yet flexible enough that they could be either dissolved in common solvents or processed in the molten state in a temperature range below the onset of decomposition. To obtain polymers having high degrees of polymerization, previously reported polymerization methods were employed:[17−33]

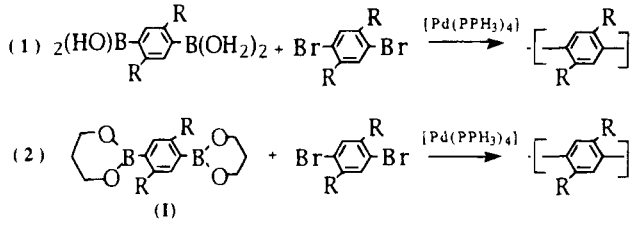

(I)

Another objective of the present investigation was to correlate the liquid crystalline behavior of poly(2,5-dodecyl-1,4-phenylene) with the degree of polymerization. Poly(2,5-dialkyl-1,4-phenylene)s are ideal model materials for the investigation of polymers that form anisotropic domains in the molten phase, due to a minimum of polar interactions. It is generally accepted for monodisperse polymers in the molten state that an axial ratio of 6.2 is necessary for the formation of the liquid crystalline state. However, for a melt containing molecular rods having a distribution of molecular lengths, phase separation of the polymer into phases containing different molecular weights may occur. The phase separation of rigid-rod polymers having a molecular weight distribution into different phases containing

[⊗] Abstract published in *Advance ACS Abstracts,* November 1, 1995.

0024-9297/95/2228-8350$09.00/0

different molecular weights has been predicted theoretically by Flory and Frost.[24,25] An example of this type of phase behavior for a thermotropic liquid crystalline polymer has recently been described by Witteler et al. for an oligomer of poly(2,5-di-*n*-dodecyl-1,4-phenylene) and a polymer of higher molecular weight.[26] The lower molecular weight poly(2,5-di-*n*-dodecyl-1,4-phenylene) showed only an isotropic phase upon melting, whereas the higher molecular weight polymer demonstrated two phases in the molten state, an isotropic phase and an anisotropic one. Mixtures of low and intermediate molecular weight polymers have been shown by Witteler et al. to even consist of three phases, where the isotropic phase coexists with two different liquid crystalline phases. The separation of rigid-rod polymers into multiple phases and its dependence on molecular weight has been confirmed experimentally for lyotropic systems.[27,28]

In an extension of the work of Witteler et al.,[26] a series of poly(2,5-di-*n*-dodecyl-1,4-phenylene)s has been synthesized having a broad range of molecular weights. Poly(2,5-di-*n*-dodecyl-1,4-phenylene) (PPP) has been synthesized of sufficiently large molecular weight such that only a single anisotropic phase is present in the molten phase, to the complete exclusion of an isotropic state. Since in any polycondensation reaction there is a distribution of molecular weights, it might be expected that, even in a polymer whose molecular weight can be described as high, there would be a fraction of low molecular weight polymer that might form a second isotropic phase. However, with increasing molecular weight, the volume fraction of polymers having low degrees of polymerization decreases, and fractionation of the polymer in the molten state into multiple phases containing different molecular weights becomes increasingly unlikely.

The principal objectives of this study include the following: (1) the synthesis of various poly(2,5-di-*n*-dodecyl-1,4-phenylene)s having a broad range of molecular weights; (2) characterization of their morphology using X-ray diffraction; (3) confirmation of their liquid crystalline phase behavior in the molten state, i.e., study of the influence of molecular weight on phase formation (principal methods for the elucidation of phase behavior included differential scanning calorimetry and rheological measurements); (4) characterization of their mechanical–dynamical behavior using dynamic mechanical measurements; (5) a preliminary investigation of the mechanical properties of high molecular weight PPPs and their correlation with relaxational phenomena.

Experimental Section

GPC measurements were conducted at 60 °C in 1,2-dichlorobenzene using a Waters 150-C ALC/GPC equipped with an external ERC 7511 infrared detector. Three successive poly(styrene–divinylbenzene) columns, PSS-SDV GEL, were used having a particle size of 10 μm and a porosity of 500, 10 000, and 100 000 Å, respectively. Solution viscosities were measured in an Ubbelohde viscometer at 85 °C in 1,2-dichlorobenzene. Inherent viscosities, molecular weights, and methods of preparation for the various poly(2,5-di-*n*-dodecyl-1,4-phenylene)s are summarized in Table 1. The various substituted poly(*p*-phenylene)s will be denoted by PPP, followed by their weight-average molar mass (g/mol × 10^{-3}).

Differential scanning calorimetry measurements were obtained at heating and cooling rates of 10 °C/min using a Mettler DSC-30 calibrated with an indium standard. Dilatometry measurements were conducted using a Gnomix research PVT apparatus at pressures of 10, 100, and 150 MPa. The coefficient of volume expansion at atmospheric pressure, α_v, was obtained by linear extrapolation. The morphologies of solution-cast and melt-pressed films were characterized by X-ray diffraction (Ni-filtered Cu Kα radiation) using a flat film camera. For powder samples, a Phillips powder diffractometer PW 1820 was used. Films were characterized at various temperatures in the reflection mode (1–40°) also using a Phillips 1820 powder diffractometer. Solution ^{1}H-NMR measurements were obtained using a Bruker AC-300 NMR spectrometer. Solid-state ^{13}C-NMR experiments were conducted on a Bruker MSL-300 using CP/MAS/TOSS. The experiments were conducted as follows: the cross-polarization time was 2.0 ms; the magic angle spinning rate was 4.0 kHz; the delay between scans was 2.0 s; the 180° ^{13}C pulse was 7.0 μs; and the 90° ^{1}H pulse was 3.7 μs.

Table 1. Methods of Preparation, Yields, GPC Analyses, and Inherent Viscosities for the Various Poly(2,5-di-*n*-dodecyl-1,4-phenylene)s Studied

polymer	method (yield)	T (°C)[a] (catalyst)[b]	M_n[c] (g mol^{-1} × 10^{-3})	M_w[c] (g mol^{-1} × 10^{-3})	M_n/M_w[c]	$[\eta]_{inh}$[d] (dL/g)
PP8		120 (0.004)	3.9	7.9	2.03	0.03
PPP22	1 (90%)	115 (0.004)	8.7	22.0	2.52	0.14
PPP29	1 (72%)	80 (0.009)	10.5	29.2	2.78	0.20
PPP44	2 (80%)	65 (0.006)	17.0	44.3	2.61	0.25
PPP73	2 (96%)	65 (0.004)	24.0	73.0	3.05	0.51
PPP95	2 (92%)	65 (0.003)	34.0	94.7	2.78	0.58
PPP116	2 (97%)	60 (0.002)	39.4	116.0	2.95	0.71
PPP137	1 (99%)	115 (0.004)	39.4	137.3	3.48	0.91

[a] Polymerization temperature. [b] Mole equivalent catalyst. [c] GPC. [d] 1,2-Dichlorobenzene, 85 °C.

Tensile measurements were obtained from solution-cast films prepared by dissolving 0.6 g of polymer in 20 mL of *p*-xylene. The solution was then heated at 50 °C in a Petri dish, and the solvent was allowed to evaporate. Upon evaporation of the solvent, the resulting polymer film separated from the surface of the substrate. The resulting films were then stamped into a dog bone shape using the form DIN 53 504.53A (Deutsche Insdustrie Norm). Tensile measurements were made at 0.1 mm/min using an Instron 6022 testing machine. Tensile values are an average of six measurements.

A Rheometrics RMS-800 rheometer was used to measure the viscoelastic response of the polymers between −120 and 300 °C. Measurements of polymer viscoelastic properties were conducted in all cases using shear deformation. Rheological measurements in the molten state were obtained using a cone and plate geometry (50 mm diameter, 1°), with the exception of temperature sweeps, in which case a parallel plate (25 mm diameter) geometry was used (5 rad/s). For rheological measurements in the molten phase, viscoelastic quantities such as G', G'', and η^*, were found to be independent of strain amplitude. For viscoelastic measurements below melting temperatures, a solution-cast film (10 rad/s, 0.3% strain) and a melt-pressed rod (5 rad/s, 0.003% strain) were prepared. **PPP116** was heated to 230 °C, after which pressure of 1 kN was applied using a Weber press, yielding a rod of 43 mm length and 5 mm diameter. The solution-cast film was prepared as previously described and had the following dimensions: 0.4 × 5.0 × 50.0 mm. Solution viscosity measurements were obtained at 50 °C in a mixture of *o*-/*p*-diethylbenzene using a Bohlin VOR rheometer. A concentric cylinder (C14) geometry was used, where the radius of the inner and outer cylinders were 7.0 and 7.7 mm, respectively.

Syntheses. A. Bis(1,3-propanediol) Ester of 2,5-Di-*n*-dodecylbenzene-1,4-diboronic acid (I). To a 1 L single-neck round-bottom flask were added 50 g of 2,5-di-*n*-dodecylbenzene-1,4-diboronic acid (99.5 mmol), 500 mL of dry methylene chloride, and 15 g of 1,3-propanediol (0.199 mol). The diboronic acid formed a suspension in methylene chloride. Methylene chloride was slowly removed by distillation (45 °C) at atmospheric pressure using a rotary evaporator. After approximately one-half of the methylene chloride was removed, 250 mL of dry methylene chloride was added. This process

was repeated until the complete dissolution of the diboronic acid occurred. Toward the end of this procedure, it may be necessary to add a small quantity of additional 1,3-propanediol. The solution was concentrated to dryness. The resulting solid was then recrystallized from dry ethyl acetate (80 mL). Yield: 70%. mp: 70–72 °C. Anal. Calcd for $C_{36}H_{64}O_4B_2$ (582.49): C, 74.23; H, 11.07. Found: C, 74.08; H, 10.93. ^{1}H NMR ($CDCl_3$): δ 0.88 (t, 6H, CH_3), 1.26 (m, 36H, $CH_2(CH_2)_9CH_2$), 1.52 (m, 4H, CH_2CH_3), 2.01 (m, 4H, $OCH_2CH_2CH_2O$), 2.75 (t, 4H, {hCH_2), 4.13 (t, 8H, OCH_2), 7.42 (s, 2H, PhH). Mass spectrum (70 eV) *m/e* (M^+ rel. intensity): 583.58 (15.9), 582.57 (44.9), 581.55 (21.4). IR/KBr (cm^{-1}): 2918 (asymmetric C–H stretch, CH_3, CH_2), 2850 (symmetric C–H stretch, (CH_3, CH_2), 1285 (B–O stretch).

B. Poly(2,5-di-*n*-dodecyl-1,4-phenylene) (PPP137). To a 500 mL three-neck round-bottom flask equipped with a reflux condenser and a 500 mL addition funnel were added 12 g (23.89 mmol) of 2,5-di-*n*-dodecylbenzene-1,4-diboronic acid (a), 17.09 g (29.85 mmol) of 1,4-dibromo-2,5-di-*n*-dodecylbenzene (b), 25.43 g of Na_2CO_3, and a magnetic stirrer. The addition funnel was separated from the round-bottom flask by an adapter containing a vacuum-tight stopcock. The apparatus was then evacuated (<1 mbar) and filled with a nitrogen atmosphere. This process was repeated four additional times, after which 0.138 g of [$Pd(PPh_3)_4$] was added. Solvents used for polymer preparation were treated and transferred so as to guarantee the strict exclusion of oxygen. Distilled water (200 mL) and toluene (120 mL) were separately refluxed for 1 h under a steady stream of nitrogen, which was bubbled into the solutions. The solvents were then cooled to room temperature and transferred to the addition funnel. In a separate apparatus, tetrahydrofuran was maintained at reflux for at least 1 h under a nitrogen atmosphere, after which 90 mL of distilled THF was withdrawn and combined with the other solvents in the addition funnel. Nitrogen was bubbled through the combined solvent mixture for an additional hour, after which the solvents were added to the reaction vessel. The addition funnel was then replaced by a rubber septum. The two-phase reaction was maintained overnight at reflux (≈120 °C oil bath temperature) using the fastest possible stirring rate. Additional quantities of diboronic acid were subsequently injected twice daily into the round-botton flask via the stopcock adapter equipped with a rubber septum. The diboronic acid was dissolved in the smallest quantity of distilled, deoxygenated THF necessary. The diboronic acid was added in the following increments: 1,5, 0.75, 0.45, 0.225, 0.075 g (1:1 a/b, 4th day), followed twice daily by 10 additional injections of 0.045 g each over a 5 day period (1.03:1 a/b, 9 days). The two-phase solution was then cooled and added to 500 mL of acetone. The precipitated polymer was filtered and twice washed in boiling water. The polymer was dried, dissolved by heating in 2 L of toluene, filtered, and precipitated into a copious amount of acetone. The collected polymer was then extracted in a Soxhlet for 1 day with acetone. As previously described, the polymer was additionally dissolved in toluene, precipitated into acetone, collected, and vacuum-dried.

C. PPP116. Unless stated to the contrary, the same procedures used for **PPP137** were applied to the preparation of **PPP116**. To a 500 mL two-neck round-bottom flask equipped with a magnetic stirrer and a 500 mL addition funnel separated by an adapter containing a vacuum-tight stopcock were added 11 g of **I** (0.0189 mol), 10.81 g of 1,4-dibromo-2,5-di-*n*-dodecylbenzene (0.0189 mmol), and 12.91 g of Na_2CO_3 (0.122 mol). The reaction vessel was evacuated and filled with nitrogen to which 43.6 mg of [$Pd(PPh_3)_4$] was added (0.002 equiv). Distilled water (115 mL), 60 mL of distilled THF, and 70 mL of toluene were then added to the reaction vessel. The two-phase solution was heated at reflux for a short period to ensure the dissolution of all reagents and then heated at 60 °C (bath temperature) for 8 days.

D. PPP8. By using the same procedure previously described for **PPP137**, 4.66 g of 2,5-di-*n*-dodecylbenzene-1,4-diboronic acid (9.27 mmol), 5.59 g of 1,4-dibromo-2,5-di-*n*-dodecylbenzene (9.76 mmol), 7.50 g of Na_2CO_3 (0.07 mol), and 0.04 g of [$Pd(PPh_3)_4$] (0.034 mmol), were added to a nitrogen-filled 500 mL two-neck round-bottom flask. After addition of the solvents, the reaction was heated at 120 °C for 2 days.[30]

Results and Discussion

Synthesis. With the objective of obtaining high molecular weight PPP, methods 1 and 2 were both investigated. Method 1 was limited by the difficulty of obtaining pure 2,5-di-*n*-dodecylbenzene-1,4-diboronic acid. The diboronic acid is a white powder likely contaminated by boronic anhydrides, thus leading to inbalances in stoichiometry. Stoichiometric polymerizations can, however, be obtained by the gradual addition (8–9 days) of 1.03 equiv of the diboronic acid to a 2,5-*n*-dialkyl-1,4-dibromobenzene. This method must be conducted at elevated temperatures to assure that a stoichiometric balance in the polymerization is obtained before an excess of diboronic acid is added. Method 2 had the advantage that the bis(1,3-propanediol) ester of diboronic acid is highly crystalline and can be readily purified, such that stoichiometric reactions could be carried out at comparatively low temperatures. This method was only limited in that one extra synthetic step was necessary, the conversion of diboronic acid to its bis(1,3-propanediol) ester. In the synthesis of polymers having high degrees of polymerization, both methods should be considered highly effective.

Polymer Morphology. The morphology of films prepared from the dodecyl-substituted poly(*p*-phenylene)s is unusual in that a high degree of orientation can be obtained, regardless of sample preparation, and in the absence of posttreatment. Whether cast from solution or obtained from the liquid crystalline melt, films prepared from these materials demonstrate a similar level of orientation. To fully characterize the structure of these materials, films were analyzed by X-ray diffraction with the X-ray beam both parallel and perpendicular to the film surface. Shown in Figure 1a,b are diffraction patterns of **PPP137** as cast from a solution of *p*-xylene: (a) the X-ray beam was perpendicular to the film surface and (b) the X-ray beam was perpendicular to the film edge. In the latter case, intense equatorial reflections indicative of high-order reflexes were observed. These reflexes (n = 1, 3, 5) correspond to the periodic structure of the materials, consisting of layers of side chains separated by layers of main chains. Because these reflexes were absent in the case where the X-ray beam was perpendicular to the film surface, it can be concluded that the structure consists of layers assuming preferential orientation parallel to the film surface, with layers of backbone chains separated by well-ordered layers of side chains. Because the X-ray diffraction pattern shows a uniform intensity distribution with respect to the azimuthal angle for films analyzed with the X-ray beam perpendicular to the film surface, the main chains can be regarded as being locally oriented, but macroscopically isotropic. Thus, when prepared from solution, the side chains can be envisioned as being located perpendicular to the substrate surface, separating layers of main chains that are spaced parallel to the substrate surface, as depicted schematically in Figure 1a,b. Melt-pressed films that were quenched from the liquid crystalline phase, as shown in Figure 2a,b show the same type of orientation observed for the solution-cast films. This indicates, regardless of the method of preparation, that there is a strong tendency for the polymer main chains to segregate from the layers of side chains, yielding a sandwich type structure.

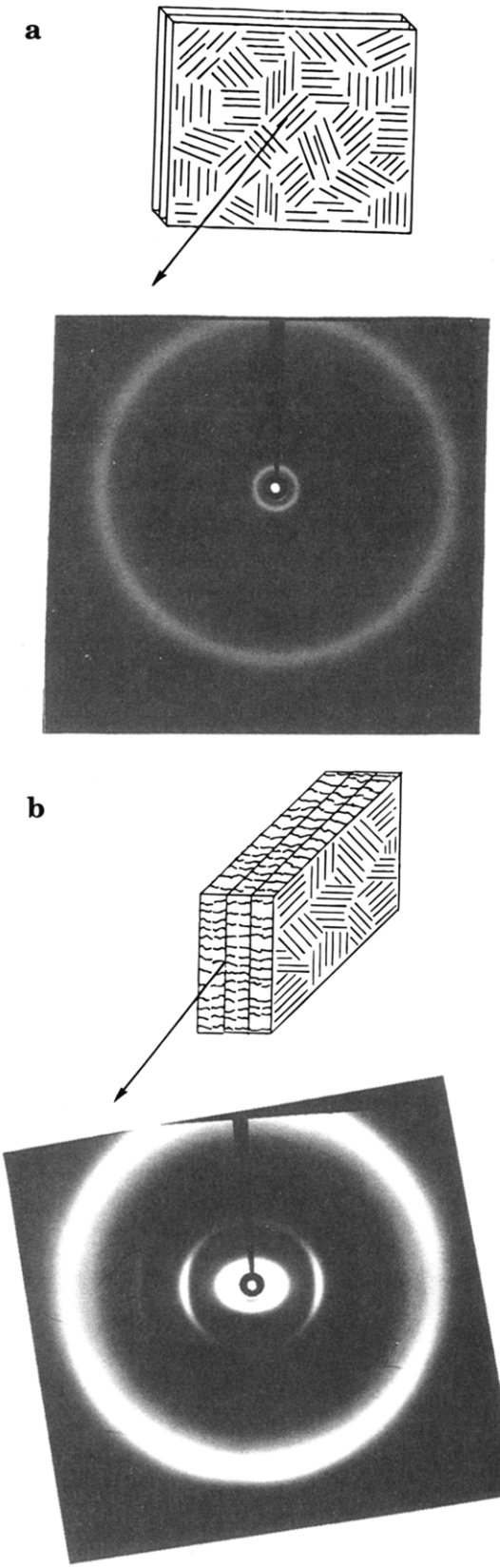

Figure 1. X-ray diffraction patterns measured for a solution-cast film of **PPP137**: (a) the film surface was perpendicular to the incident beam; (b) the X-ray beam was parallel to the film edge.

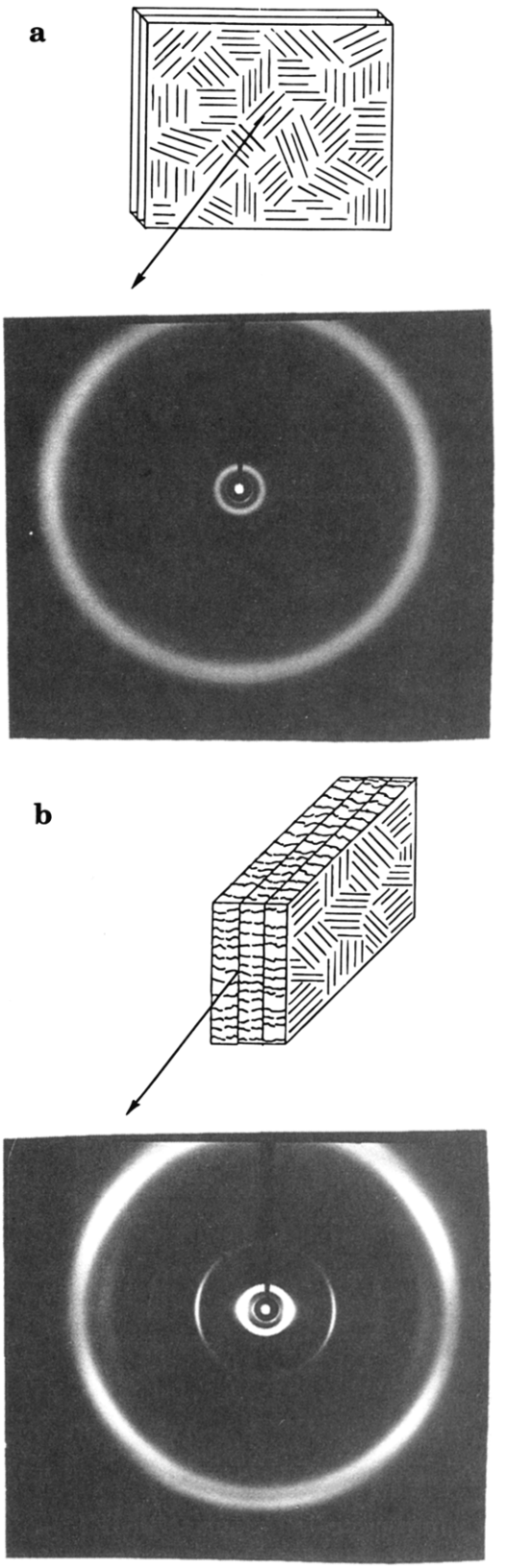

Figure 2. X-ray diffraction patterns measured for a melt-pressed film of **PPP137**: (a) X-ray beam perpendicular to film surface; (b) X-ray beam parallel to film edge.

The morphologies present in both the solution-cast and melt-pressed films were also investigated at elevated temperatures. Shown in Figure 3 are the X-ray intensity distributions for the solution-cast films with increasing temperature **(PPP137)**. No appreciable deviation was observed for the corresponding melt-pressed films. The higher order reflexes, $n = 1, 3, 5$ (34.6, 11.4, and 6.9 Å; room temperature), which correspond to the layer spacing of the side chains, show only a small dependence on temperature until polymer melting. As shown in Figure 4, the layer spacing of the side chains decreased linearly with increasing temper-

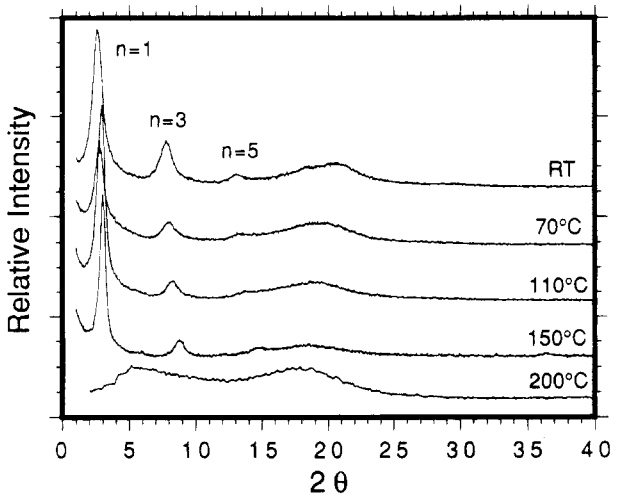

Figure 3. X-ray diffraction intensity distributions measured at various temperatures for a solution-cast film of **PPP137**.

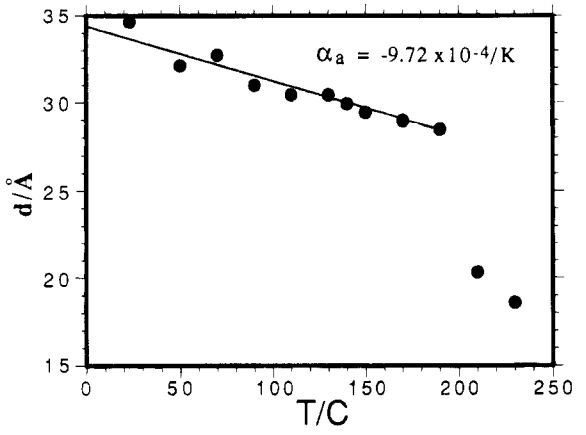

Figure 4. Layer spacings (d) for a solution-cast film of **PPP137** measured at various temperatures.

ature until polymer melting. The decrease in the layer spacing of the side chains with increasing temperature is an unusual result, yielding a large negative coefficient of thermal expansion ($\alpha_a = -9.72 \times 10^{-4}$/K). A negative thermal expansion coefficient for the layer spacing of the side chains is consistent with previously reported work on poly(2,5-bis(hexadecyloxy)-1,4-phenyleneterephthalate), which is also a rigid-rod polymer containing long side chains.[29] The broad, weak reflections that can be observed at higher angle, 9−11°, correspond to the packing of the side chains. In previous work on samples annealed at 170 °C and then cooled to room temperature, it was shown that the side chains ideally lie almost perpendicular to the main chains in an orthorhombic type packing.[30] Because the reflections from which the orientation of the side chains could be deduced are both weak and diffuse, it can be concluded for the films, both melt-pressed and solution-cast, that the packing of the side chains contains various defects.

The structural changes observed by X-ray diffraction with increasing temperature can be correlated to transitions observed by differential scanning calorimetry. Shown in Figure 5 are the second heating and cooling traces of **PPP137**, the polymer having the highest molecular weight, and **PPP8**, an intentionally prepared oligomer[30] representing the lowest molecular weight. The second heating and cooling curves were used to assure that all samples possessed the same sample history. Upon heating from room temperature, very broad endotherms were typically observed in the DSC

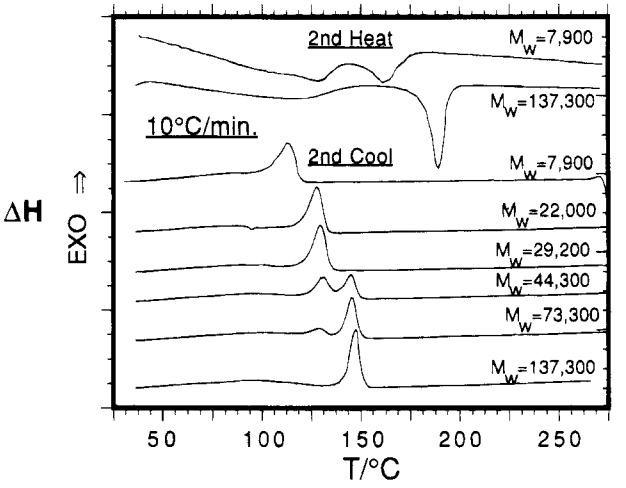

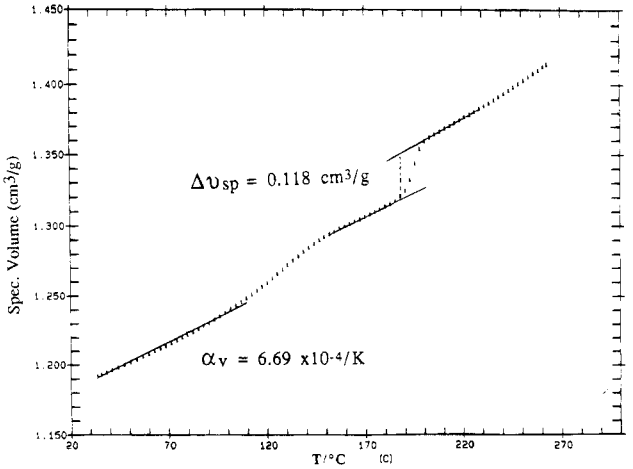

Figure 5. (a) Molecular weight dependence of the heating and cooling DSC scans for selected PPPs (10 °C/min). (b) Corresponding plot of the specific volume versus temperature for **PPP137**.

for all polymers investigated, between 50 °C and main chain melting. The broad endotherms likely represent the deviation of the side chains from the more stable trans conformation to a side chain organization having an increasing content of gauche conformations with increasing temperature. However, because sharp reflections observed by X-ray diffraction and attributable to the layer spacing of side chains are still present at temperatures greater than 170 °C, a complete loss of order between the main chains does not occur, perhaps indicating that the final melting of the side chains coincides with the melting of the main chains. As shown in Figure 5, the melting of the main chain for **PPP137** occurs at 188 °C, while the melting temperature of the oligomer occurs at an appreciably lower temperature (161 °C) and overlaps the broad relaxation of the side chains.

In the molten state, the molecular ordering of the polymer chains was molecular weight dependent. As observed by polarizing optical microscopy, the low molecular weight polymers formed an isotropic melt. Polymers having intermediate molecular weights, **PPP44** and **-73**, showed a two-phase texture, an anistropic LC phase and an isotropic phase, with the relative amounts of the two phases being dependent on both the molecular weight and its distribution.[26] Upon further heating of **PPP44** or **−73** until the onset of significant polymer degradation (>320 °C), the LC phase component remained a stable and separate phase. Polymers having

the highest molecular weights showed only a single liquid crystalline texture, which was stable at elevated temperatures until polymer decomposition. The formation of these phases in the molten state was reflected in their second DSC cooling scans. Polymers having the highest molecular weights, such as **PPP137**, showed only a single exotherm upon cooling from the molten phase, which for **PPP137** occurred at 147 °C at the selected cooling rate of 10 °C/min. For polymers of intermediate molecular weight, **PPP44** and **-73**, two separate crystallization exotherms were observed upon cooling from the molten state: crystallization of the LC component of the molten state followed by crystallization of the isotropic component, which occurred at lower temperature. As indicated by single low-temperature crystallization exotherms upon cooling from the molten state and by the lack of an anisotropic molten phase, as observed by polarizing optical microscopy, it can be concluded for the lower molecular weight polymers, **PPP8**, **-22**, and **-29**, that crystallization occurred only from an isotropic melt. Consequently, the DSC can be used as a rough guideline to establish the relative amounts of the isotropic and anisotropic phases in the molten state for these polymers.

Shown in Figure 5b is the temperature dependence of the specific volume of **PPP137**. From measurements of specific volume with increasing temperature at various pressures, the coefficient of volume expansion in the temperature range between room temperature and 120 °C was obtained ($\alpha_v = 6.69 \times 10^{-4}$/K). By using the coefficient of thermal expansion for the direction perpendicular to the main chains, which corresponds to layer spacing of the side chains ($\alpha_a = -9.72 \times 10^{-4}$/K), and by assuming that thermal expansion along the *p*-phenylene backbone is negligible ($\alpha_b = 0$), the coefficient of thermal expansion for the direction lateral to the main chains could be obtained: $\alpha_c = 1.64 \times 10^{-3}$/K. These results indicate that, during heating in the temperature regimes investigated, positive thermal expansion of the polymer occurred only in the direction lateral to the main chains.

The change in specific volume upon polymer melting was 0.118 cm^3/g (10 MPa). In the molten phase, the coefficient of volume expansion could be described by $V_{sp}(T) = V_0(Tr) + \alpha_1 T + \alpha_2 T_2$, where α_1 and α_2 are 7.59×10^{-5}/K and 1.68×10^{-6}/K, respectively (10 MPa).

Solution-Cast Films. Figure 6 shows the stress–strain curves at various temperatures for solution-cast films of **PPP137** under tensile deformation. For films deformed at room temperature, stress increased linearly with elongation until an elongation of approximately 4.28%, where brittle fracture occurred. The stress–strain curves obtained at room temperature are similar to stress–strain curves normally obtained from oriented polymer fibers or glassy polymers. However, for a glassy polymer, a brittle to ductile transition would be expected with increasing temperature accompanied by a corresponding change in the stress–strain curve. As shown in Figure 6, with increasing temperatures, the stress at break and the tensile modulus decreased significantly with increasing temperature. However, in all cases the stress increased linearly with elongation, thus satisfying the criterion of a Hookean solid. The stress–strain curves showed only a small range of nonlinearity prior to fracture, which might be attributed to small changes in polymer orientation. Shown in Figure 7 is the temperature dependence of the stress at break and the tensile modulus. The tensile properties show a linear dependence on temperature, with E, $\sigma_b \approx T^{-1}$. As previously observed by X-ray diffraction, the polymer structure can be regarded as consisting of two phases, that is, layers of stiff chains separated by layers of side chains. As shown in Figure 4, with increasing temperature a steady decrease in the layer spacing of the side chains occurred, suggesting conformational changes in the side chains from the trans to the gauche form. As will be shown subsequently by solid-state NMR measurements, deviation from the all-trans conformation begins at temperatures lower than room temperature. Consequently, the linear dependency of the tensile properties with $1/T$ might be correlated with the unusual behavior of the material with regard to thermal expansion, i.e., the gradual changes in conformation of the side chains with increasing temperature.

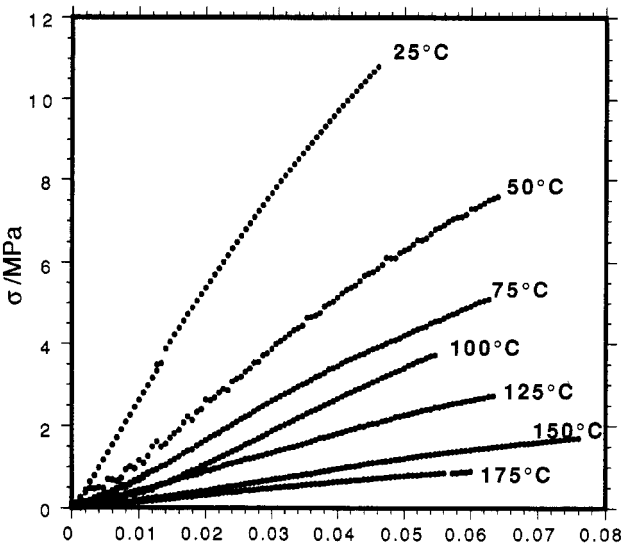

Figure 6. Stress–strain curves for solution-cast films of **PPP137** measured at various temperatures.

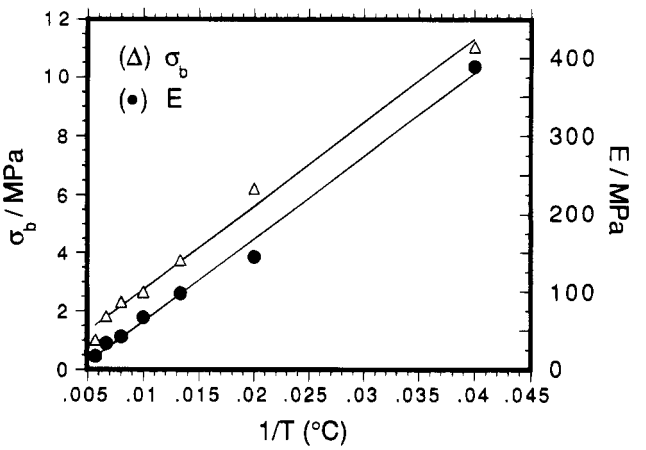

Figure 7. Temperature dependence of the stress at break (σ_b) and the tensile modulus (E) for solution-cast films of **PPP137**.

As summarized in Table 2, the elongation at break was surprisingly low for these undrawn samples, 4–6%, and does not appear to be temperature dependent. As previously determined from X-ray diffraction studies, perpendicular to the film surface the main chains were microscopically highly ordered with respect to the individual domains, yet across many domains they were isotropically ordered. Attempts to improve the orientation of the solution-cast films by posttreatment, using various temperatures, loads, and solvent treatment, were unsuccessful. These results indicate that a spon-

Table 2. Temperature Dependence of the Tensile Modulus (E), Stress at Break (σ_b), and Elongation at Break (e_b) for SolutionhCast Films of PPP137

T (°C)	σ_b (MPa)	E (MPa)	e_b (%)
25	11.05	389.06	4.28
50	6.21	144.35	5.78
75	3.74	97.96	4.28
100	2.66	66.91	4.15
125	2.31	42.06	6.21
150	1.82	26.35	6.30
175	1.01	17.04	6.23

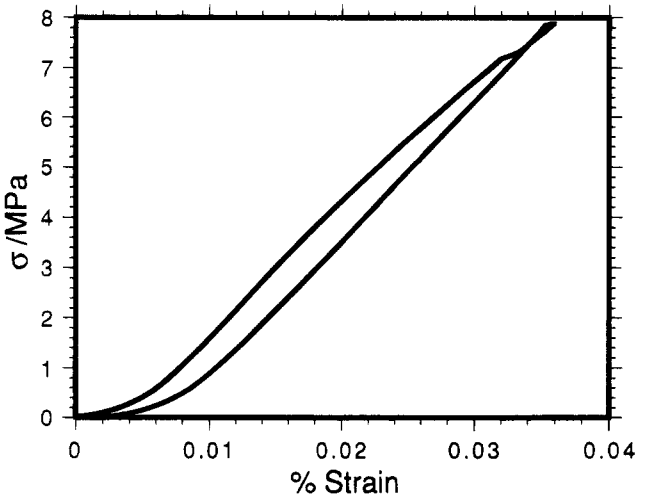

Figure 8. Response of a soluiton-cast film prepared from **PPP137** to linearly increasing tensile deformation followed by an incremental decrease in elongation.

taneous ordering of the polymer chains occurred during solvent casting, in which a uniaxial orientation normal to the substrate surface is fixed and after which the orientation cannot be readily changed.

To further study the Hookean characteristics of these polymers, a measurement of recoverable deformation was performed. Films were stretched in tension to a stress of 8 MPa, after which the stress was reduced incrementally. As shown in Figure 8, the film returned to its original length, showing a permanent deformation of 0.13%. This indicates that, prior to brittle fracture, **PPP137** demonstrates elastomeric properties that are consistent with both glassy polymers and oriented polymer fibers when subjected to small deformations.

Viscoelastic Properties. By using two methods of sample preparation, dynamic mechanical measurements were performed for polymers having the highest molecular weights: (a) **PPP137** as cast from solution and (b) **PPP116** as pressed from the melt. As shown by Figure 9, three relaxation processes can be identified. The three relaxation processes are assumed to relate to the following transitions: (1) the α transition to the global mobility of the polymer main chain; (2) the β transition to conformational changes within the side chains, that is, gradual deviation from the all-trans state to a side chain organization containing increasingly larger contents of gauche conformations with increasing temperature; and (3) the γ relaxation process, which is likely related to the onset of short-segment motions in the side chains.

As shown in Figure 9, there does not appear to be an appreciable difference in the α and β transitions for **PPP116** and **PPP137**, regardless of polymer preparation. In evaluating the α relaxation, samples were studied by dynamic mechanical measurements in the melt using cone and plate geometry, the results of which

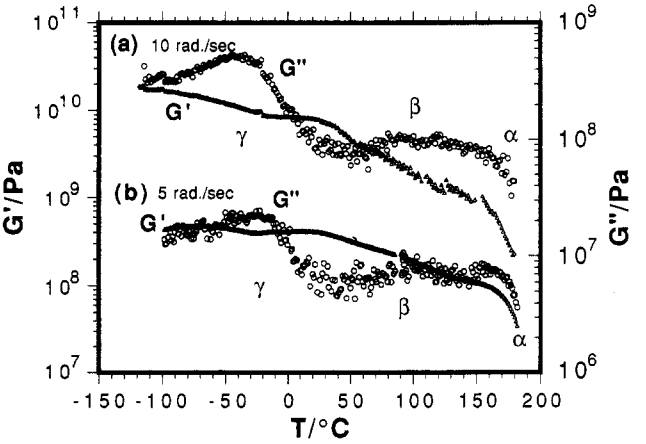

Figure 9. Temperature dependence of G' and G'' for (a) a solution-cast film prepared from **PPP137** and (b) a melt-pressed rod prepared from **PPP116**.

will be discussed in a later section. The significant decrease in the tensile properties between 25 and 50 °C can be correlated to the onset of the β relaxation, as indicated by a loss in magnitude of G' of half a decade for both **PPP116** and **-137**. The continued loss in magnitude of G' at even higher temperatures is consistent with the corresponding decrease in tensile properties. The γ transition for both polymers appeared remarkably similar for both samples, although the γ transition was shifted by approximately 10 °C to higher temperature for the sample pressed in the melt, suggesting a somewhat larger degree of mobility for the sample obtained from the melt. The γ transition corresponds to a temperature at which the first hints of side chain mobility can be observed, as suggested by solid-state NMR experiments.

The difference in magnitudes of the storage and loss moduli for the solution-cast film and the melt-pressed rod may be attributed to many factors. These include differences in sample geometry, frequency, deformation amplitude, orientation, and the fact that a shear deformation rather than a tensile deformation was employed. Consequently, conclusions based on the relative magnitudes of the storage and loss moduli for both samples are not reasonable given the present level of information.

The γ and β relaxations observed from dynamical mechanical measurements can be correlated with measurements obtained from solid-state ^{13}C NMR. Shown in Figure 10 are the solid-state spectra of **PPP116** measured at various temperatures. In the aliphatic region of the spectrum, three well-defined peaks were observed at 14.7, 24.4, and 32.8 ppm. These peaks can be assigned to the methyl carbon atom, its adjacent methylene carbon, and (the peak with the greatest intensity) the remaining side chain methylene carbon atoms. To understand the differences in the spectra obtained between −50 and 100 °C, reference is made to poly(ethylene) and other rigid-rod polymers containing aliphatic side chains.[31-34] Poly(ethylene) shows a peak at 34.4 ppm, which has been attributed to methylene units lying in the crystalline regions having the trans conformation. An additional peak is observed for poly(ethylene) at 32.0 ppm, which has been attributed to methylene carbons located in the amorphous regions having the gauche conformation. In this case, at −50 °C only a single peak can be identified at 32.8 ppm, which suggests that at this temperature the all-trans conformation is dominant. A slight deviation from the

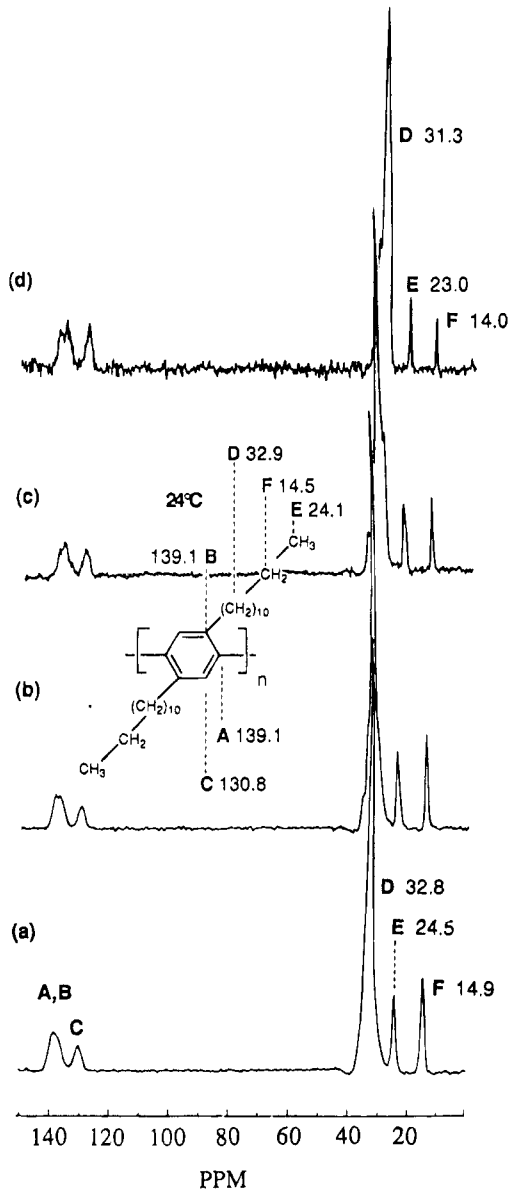

Figure 10. CP/MAS/TOSS ^{13}C-NMR spectra of **PPP116** measured as a function of temperature: (a) −50, (b) 0, (c) 50, and (d) 100 °C.

structure obtained at −50 °C is observed at 0 °C, as seen by the broadening of the peak and the appearance of other signals. Thus, the γ relaxation observed from dynamical mechanical measurements likely represents the onset of mobility for the polymer side chains.

Between 0 and 50 °C the growth of other peaks can be clearly observed, yet no appreciable frequency shift in the peak maximum occurred. Side chain mobility dramatically increased as 100 °C was reached, as suggested by a frequency shift from 32.3 to 31.3 ppm for the internal side chain carbon atoms, a shift from 24.2 to 23.0 ppm for the methylene carbon atoms located adjacent to the methyl carbon atom, and a shift from 14.5 to 14.0 ppm for the methyl carbon atoms. These results suggest that the β relaxation likely represents the transition from predominantly trans conformations to a side chain organization having an appreciably larger gauche content than that at room temperature. However, because the layer spacing, as shown in Figure 4, does not abruptly decrease, a gradual increase in the content of gauche conformations can be assumed for the β relaxation.

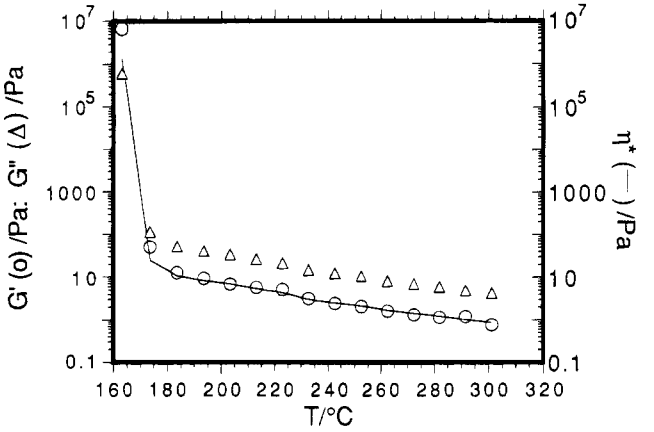

Figure 11. Temperature dependence of η^*, G', and G'' for **PPP137** in the molten state.

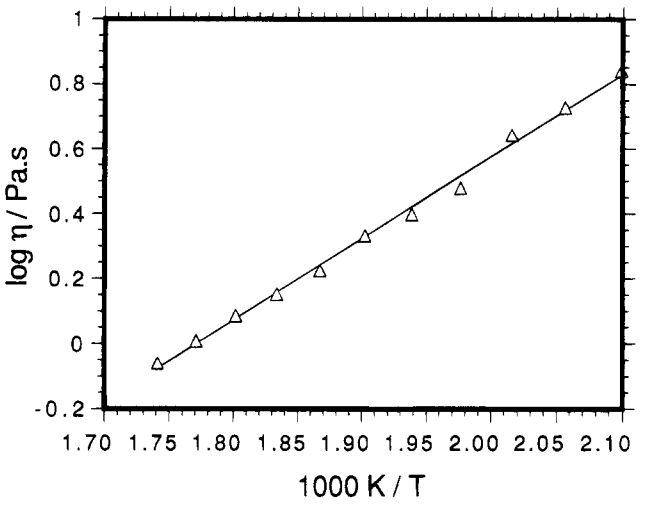

Figure 12. Arrhenius fit for the temperature dependence of η for **PPP137**.

Rheological Behavior. In the molten state, the polymers were also studied by dynamic mechanical measurements using two types of sample geometries. For measurements of the temperature dependence of polymer viscosity over a broad temperature range, measurements were conducted using a 0.4 mm layer of polymer between parallel plates. The temperature dependence of η^*, G', and G'' (10 rad/s) for **PPP137** is shown in Figure 11. **PPP137** was cooled from 300 °C until the onset of crystallization, as shown by the rapid transition to higher viscosity and higher moduli. As indicated by the DSC traces for **PPP137** (Figure 5), a single stable liquid crystalline phase existed between polymer melting and polymer degradation. This is confirmed by the lack of a transition in η^*, G', and G'' between polymer melting and polymer degradation. For polymers incapable of forming an anisotropic phase, **PPP8** for example, the temperature dependence of η^*, G', and G'' was similar to that observed for **PPP137**, in that no other transitions were observed with increasing temperature between polymer melting and polymer degradation.

The temperature dependence of the viscosity for **PPP137**, as shown in Figure 12, corresponds well to an Arrhenius type relationship typical of Newtonian fluids. From a plot of log η versus $1/T$, an activation energy of 20.9 kJ/mol was calculated. This activation energy is consistent with many values obtained for flexible polymers such as poly(ethylene) (25 kJ/mol).[36]

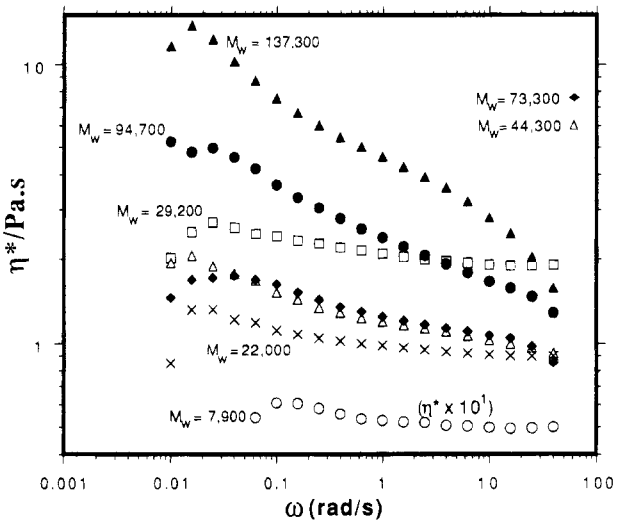

Figure 13. Frequency dependence of G', G'', and η^* for substituted poly(*p*-phenylene)s having a broad range of molecular weights (200 °C).

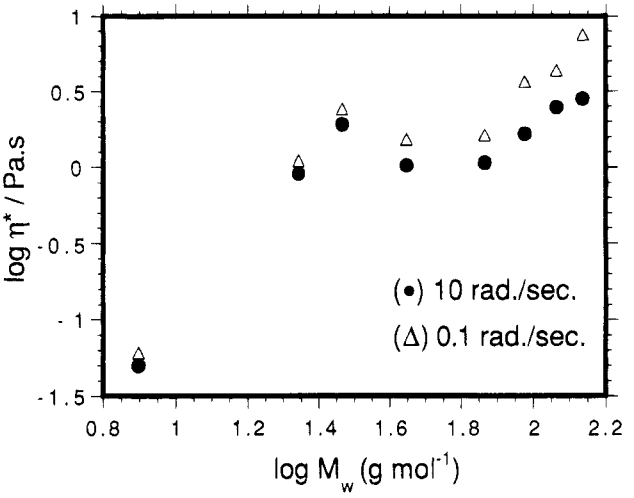

Figure 14. Molecular weight dependence of η^* at 0.10 and 10.0 rad/s, measured at 200 °C.

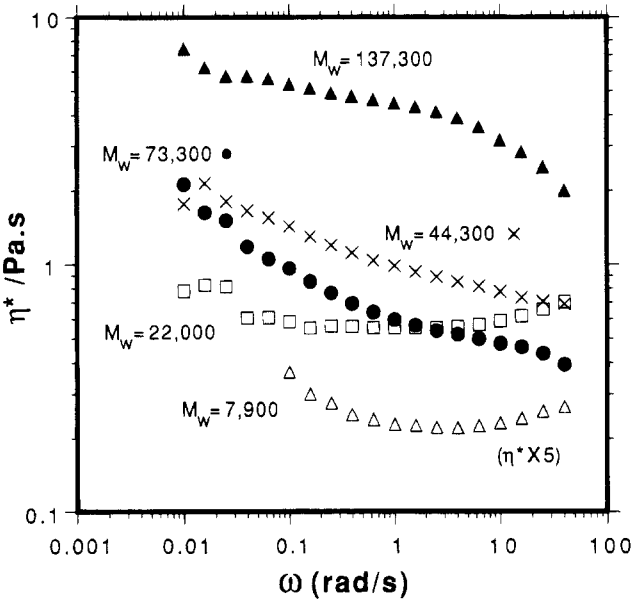

Figure 15. Frequency dependence of G', G'', and η^* for various substituted poly(*p*-phenylene)s, measured at 250 °C.

Of primary interest in this investigation was the molecular weight dependence of the viscosity. Because of the low viscosity of liquid crystalline materials, cone and plate geometry was necessary to obtain reliable viscoelastic data (η^*, G', G'') at low shear rates. Figure 13 shows the frequency dependent viscosity at 200 °C for polymers having a broad range of molecular weights. For the low molecular weight polymers, **PPP22** and **-29** and the oligomer **PPP8**, behavior typical of a Newtonian fluid was observed, that is, the viscosity was independent of the deformation frequency. This is consistent with data from DSC, which indicated, upon cooling from the molten state, that only crystallization from an isotropic phase occurred. However, for samples of higher molecular weight, the viscosity was observed in all cases to be highly dependent on deformation frequency, displaying behavior typical of a shear thinning non-Newtonian fluid. For polymers that have been shown by DSC and POM to have two phases in the molten state, an isotropic and an anisotropic phase, **PPP44** and **-73**, the viscosity was observed to be lower at all deformation rates than that of polymer **PPP29**, a lower molecular weight polymer that formed only an isotropic melt. For **PPP137**, which formed only a one-phase anisotropic melt, the decrease in polymer viscosity with increasing shear rate was 1 order of magnitude over the frequency range measured. A comparison of the molecular weight dependence of the viscosity at 0.1 and 10.0 rad/s is shown in Figure 14. For the polymers that exclusively formed anisotropic melts, the viscosity was appreciably lower at the higher deformation frequency.

As shown in Figures 15 and 16, dynamic mechanical measurements conducted at 250 and 300 °C showed the same molecular weight dependence. At all temperatures measured, **PPP137** demonstrated behavior consistent with a shear thinning non-Newtonian fluid. The effect of temperature seemed to have a small influence on the shear rate dependence of the viscosity in the terminal zone. At 300 °C, for polymers that formed anisotropic melts, polymers **PPP137** and **-44**, the viscosity seemed to decrease at a faster rate than at 200 °C. **PPP44**, for example, with increasing shear rate, reached a plateau in viscosity at 0.1 rad/s at 300 °C, whereas at 200 and 250 °C the viscosity continued to decline at 15 rad/s. However, because 300 °C is a temperature that approaches polymer degradation, conclusions should be considered tentative.

One objective of the present investigation was to assess the molecular weight dependence of the zero-shear rate viscosity. The zero-shear rate viscosities were calculated in accordance with the following equation, which was previously reported to describe non-Newtonian flow, where a is a constant that reflects the extent of non-Newtonian flow, b is a lateral shift factor, and τ is described as the characteristic relaxation time:[37]

$$\ln \eta/\eta_0 = (\eta/\eta_0 - a) \ln[1 + (\gamma\tau)^b]$$

Shown in Figure 17 is the molecular weight dependence of the zero-shear rate viscosity. A clear transition can be observed in the molecular weight region where both anisotropic and isotropic phases coexist in relatively equivalent amounts as confirmed by the second DSC cooling curve of **PPP44**. For the polymers whose melts consisted of only an isotropic phase, the viscosity showed the following molecular weight dependence: $\eta_0 \sim M_w^{2.9}$. An exponent of 2.9 for the low molecular weight

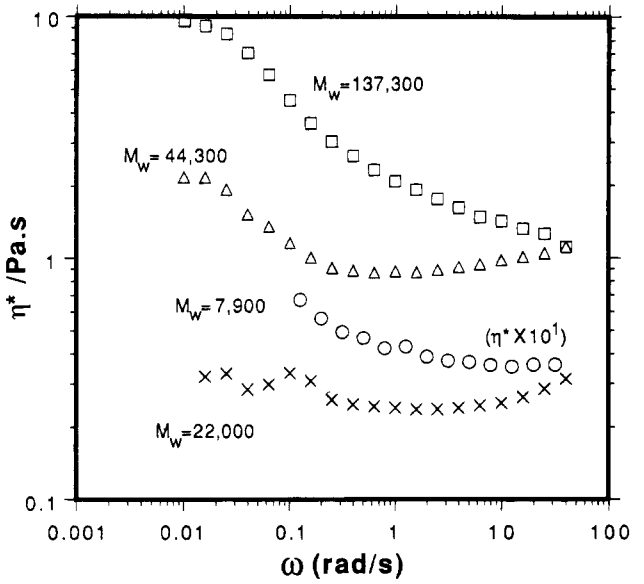

Figure 16. Frequency dependence of G', G'', and η^* for various substituted poly(*p*-phenylene)s, measured at 300 °C.

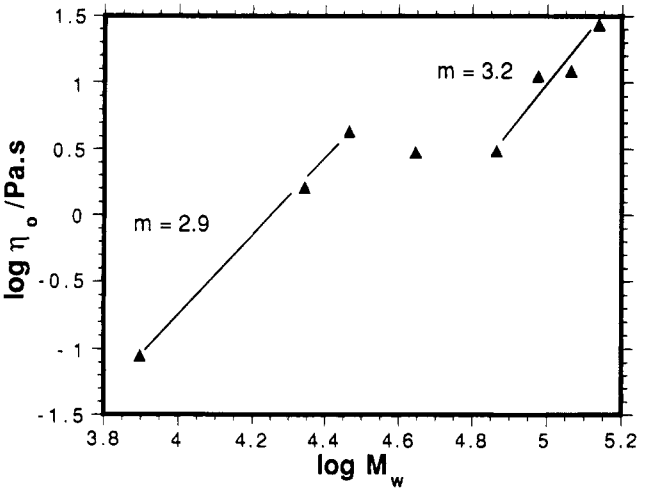

Figure 17. Molecular weight dependence of the zero-shear rate viscosity for measurements conducted at 200 °C.

polymers is significantly higher than the values normally obtained for low molecular weight polymers in the absence of molecular entanglements ($\eta_0 \sim M_w^{1.0}$). On the other hand, the chain length dependence of viscosity is much weaker than expected for concentrated or even semidiluted solutions of thin rod-like molecules i.e., $\eta \propto M^9$. The deviation of our result from these two extreme cases seems to be reasonable because the chains studied can neither be considered as flexible linear chains nor as thin rods.

An estimation of dimensions and shapes of the chains under investigation can be obtained by means of the following qualitative consideration. As indicated by $M_n/M_w > 2$, for all systems studied, there are broad distributions of chain lengths that can be represented schematically by dependencies shown in Figure 18. The POM observations and the DSC measurements (see Figure 5) both indicated that the mesophase starts to form with the sample **PPP44** (M_w = 44 000) and that the fractions of isotropic and anisotropic phases are comparable in this sample. If we assume that the microphase is formed by a fraction of chains having dimensions with the aspect ratio exceeding the critical value of 6, we could estimate the length of chains lying in approximately the middle of the chain length distribution of this sample. Considering that the diameter of the chains studied, at high temperatures, is about 2.0 nm (as determined from the low angle X-ray diffraction peak, see Figures 3 and 4), we can expect that the chains in the middle of the length distribution for this sample have approximately a critical length of 12 nm. This allows us to relate the chain length scale to the molecular weight scale, as illustrated in Figure 17. Such a consideration shows that the aspect ratio for chains in the sample **PPP7.9** is about 1, and the chains in this sample should be regarded as stars rather than rods. For samples with increasing M_w, the aspect ratio will increase, reaching the mean value of about 19 for the sample **PPP137** with the highest molecular weight.

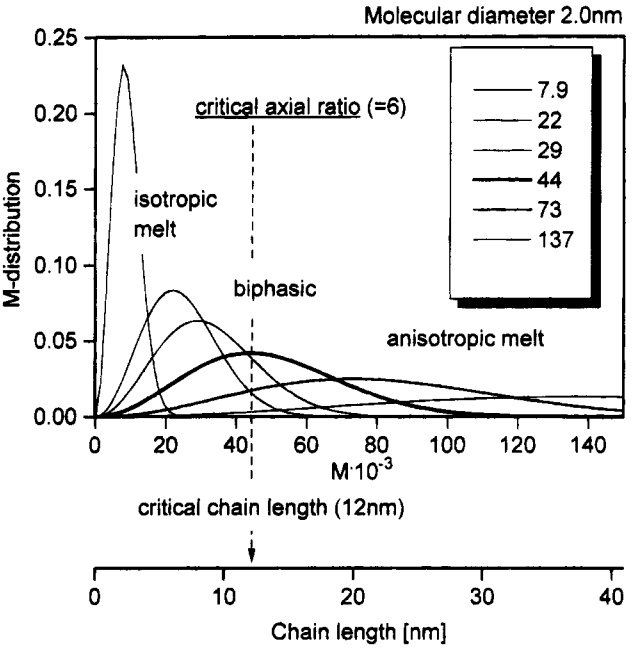

Figure 18. Most probable chain length distribution relating to samples investigated in this work; the weight averages as indicated in the figure have been determined by GPC (see Table 1).

This shows that, within the range of short chains, the nature of chains changes from starlike to hairy-rod-like. There is still a lack of a theory that would describe the rheological behavior of such systems. For longer hairy rods, where the mesophase starts to form, the viscosity drops with respect to the dependence for short chains, indicating the flow thinning effect. For polymers that showed only anisotropic melts, **PPP73**, **-95**, **-116**, and **-137**, the viscosity showed the following molecular weight dependence, $\eta \propto M_w^{3.2}$, which is surprisingly close to the dependence expected for a melt of high molecular weight entangled chains ($\eta \propto M^{3.4}$), but is much weaker than the dependence predicted for nematic phases formed in concentrated solutions of rodlike chains. It shows that the nematic phases of hairy rod molecules also require specific theoretical considerations.

These results, as well as the discussion, should, however, be considered tentative because the molecular weights of the polymers studied were determined by GPC according to polystyrene standards and not by an absolute method. The assignment of the length scale to the M_w scale (Figure 18) suggests that the molecular weights determined by GPC are probably overestimated.

An additional objective of this investigation was to determine the relaxation time of these shear thinning non-Newtonian melts after the cessation of shear de-

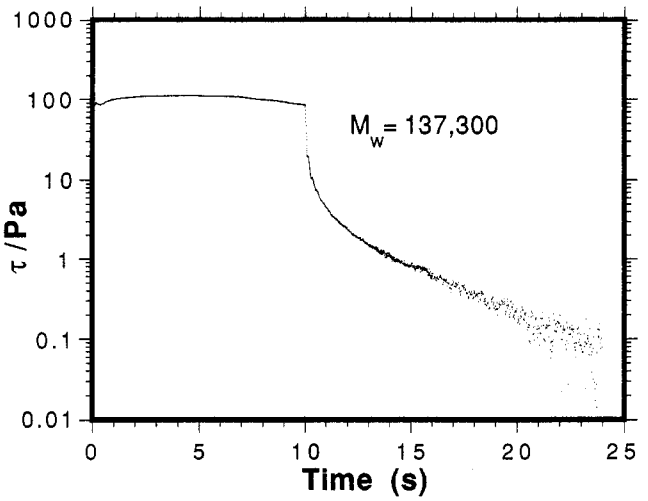

Figure 19. Stress relaxation of **PPP137** after a 10 s deformation of 10 rad/s at 200 °C.

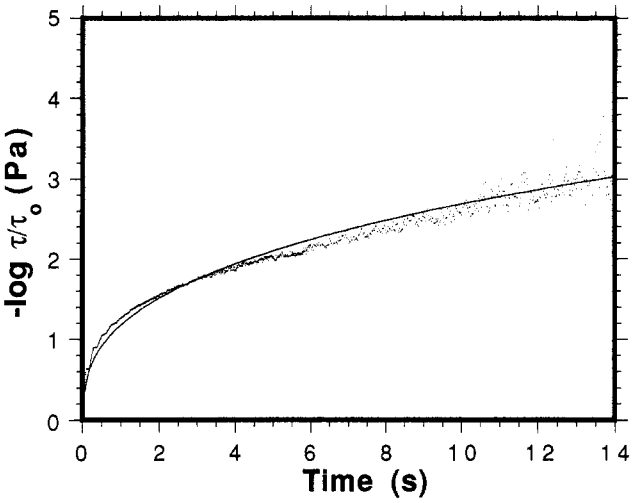

Figure 20. Fit of a stretched exponential relaxation function to a stress relaxation experiment for **PPP137**.

formation. Stress relaxation experiments were conducted in which the samples were deformed for 10 s at 10 rad/s, after which the deformation abruptly ceased. The decay of the shear stress for **PPP137** is shown in Figure 19. As shown in Figure 19, relaxation occurred very quickly. The decay in shear stress with time was fitted to the following stretched exponential relaxation function, $\sigma = \sigma_0 \exp(-t/\tau_0)\beta$, and is shown in Figure 20. For polymer **PPP137**, a relaxation time of 0.85 s was obtained ($\beta = 0.36$). Similar results were obtained for polymers **PPP95** and **PPP44**: 0.91 ($\beta = 0.30$) and 0.78 s ($\beta = 0.32$), respectively. According to the polydomain theory,[38] at low shear rates a LC polymer melt can be considered as a polydomain structure, where the many domains and their directors can be viewed as macroscopically disordered. However, a high degree of local order can exist within the LC domains, as is typical for nematic and smectic melts. At higher shear rates, it is probable that the alignment of the domains increases such that the level of molecular order can be described as macroscopic rather than local. It is probable that the relaxation times measured represent the relaxation of large, oriented domains (a monodomain structure) obtained by shearing to smaller, locally oriented domains (a polydomain structure), which are stable in the absence of flow.

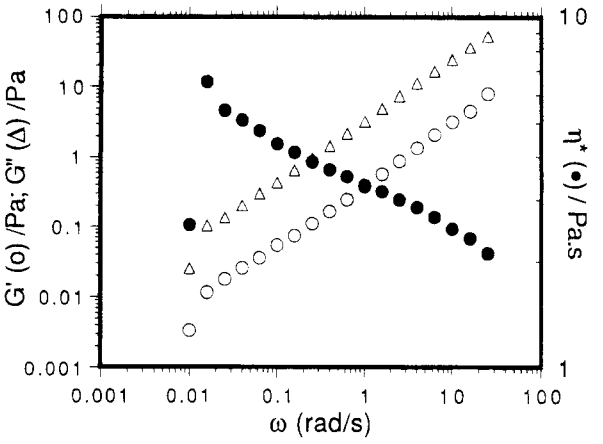

Figure 21. Frequency dependence of G', G'', and η^* for **PPP116** (200 °C).

The frequency dependence of G' and G'' may support the notion that the flow behavior of these materials is dependent on the frequency dependent reorganization of liquid crystalline domains having a distribution of sizes. As shown in Figure 21 for polymer **PPP116**, the frequency dependence of G' and G'' is not typical of Newtonian behavior. G' and G'' for Newtonian fluids have defined slopes in the terminal zone, in which G' and G'' are not parallel. In a region extending over 2.5 decades, the following frequency dependence was observed: $G', G'' \sim \omega^{0.90}$. This parallel relationship of G' and G'' was observed for all substituted poly(*p*-phenylene)s having molecular weights of 73 300 or greater. Such a parallel relationship between G' and G'' has been previously observed only in rare cases: (1) polystyrene μ networks,[39] (2) comb-shaped polymers,[40] (3) randomly branched polystyrenes,[41] (4) and for networks where the cross-linking reaction was stopped upon gelation.[42] In the case of the polystyrene μ networks, such behavior might be attributed to the "fractal" nature of the materials, in that the network consists of a large distribution of cross-links having a broad spectrum of relaxation times. The unusual behavior of the substituted poly(*p*-phenylene)s might be attributed to a distribution of domain sizes also having a broad distribution of relaxation times. This is also reflected in the low value of the β parameter of the stretched exponential function fitted to the stress relaxation curve.

The shear thinning non-Newtonian behavior of the anisotropic melts was also reflected in measurements of thixotropy, that is, the time dependent shear thinning of a liquid at increasing shear rate and corresponding shear stress, followed by gradual recovery after removal of the shear stress. In this experiment, the samples were deformed continuously at a deformation rate that increased linearly with time, after which the deformation rate was reduced in a similar manner. As shown in Figure 22, **PPP29** showed behavior consistent with that of a Newtonian liquid, in that the shear stress increased and decreased linearly with increasing and decreasing shear rate. For **PPP44**, a polymer whose melt contained both isotropic and anisotropic phases, thixotropy was observed. With increasing shear rate, the corresponding increase in shear stress declined, followed by recovery after removal of the shear stress. Unlike the behavior of **PPP29** and **PPP44**, the flow behavior for **PPP137**, the highest molecular weight polymer that formed only on anisotropic melt, can only be described as unstable. The behavior of **PPP137** is

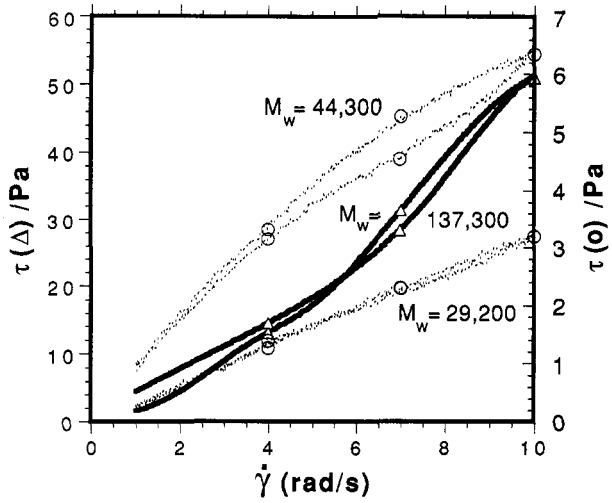

Figure 22. Dependence of the shear stress first on a linearly increasing shear rate and then a linearly decreasing shear rate for polymers **PPP29**, **-44**, and **-137** (200 °C).

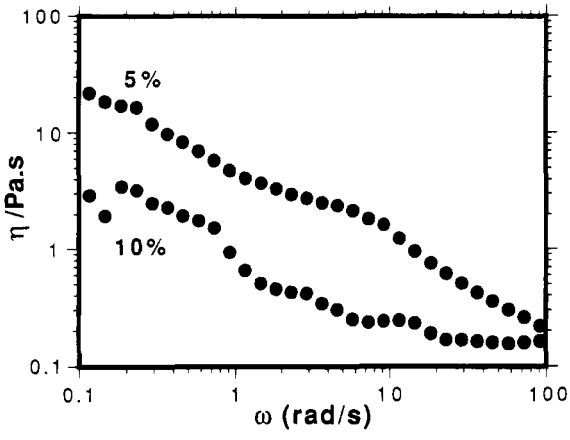

Figure 23. Frequency dependence of the viscosity η for 5 and 10% solutions of **PPP137** in *o*-/*p*-diethylbenzene at 50 °C.

characteristic of uncontrollable flow where both thixotropy and rheopexy (antithixotropy) ocurr simultaneously. Rheopexy is characterized by behavior in which the shear stress shows an increasingly positive slope with increasing shear rate and a corresponding increase in viscosity with increasing shear rate.

The shear thinning non-Newtonian behavior that was observed in the molten state was also observed for these polymers in solution. Shown in Figure 23 is the solution behavior of **PPP137** dissolved in a mixture of *o*-/*p*-diethylbenzene as measured at 50 °C. For both 5 and 10% polymer concentrations, the viscosity of the solutions decreased significantly with increasing shear rate. In view of the fact that the viscosity demonstrated such a steep dependence on the shear rate at a concentration of 5%, it can be inferred that the formation of lyotropic liquid crystalline state for **PPP137** occurs at a concentration lower than that previously reported for a carboxylic acid-substituted poly(*p*-phenylene).[22]

Conclusions

Poly(2,5-di-*n*-dodecyl-1,4-phenylene)s were synthesized in a broad range of molecular weights. As indicated by DSC, rheological measurements, and polarized light microscopy, the formation of an anisotropic phase upon melting was molecular weight dependent. As predicted by Flory and Frost for rigid-rod polymers having a distribution of molecular lengths, in the molten phase, phase separation of the rigid rods occurred. The highest molecular weight polymers formed only an anisotropic phase, to the complete exclusion of an isotropic phase. Polymers of intermediate molecular weight were biphasic, containing both isotropic and anisotropic components in the molten phase. Polymers of low molecular weight showed only an isotropic phase. Phase separation of the polymer chains was not limited, however, to the phase separation of the high molecular weight component of the polymer into anistropic domains and the lower molecular weight component into isotropic domains. Phase separation also occurred on the microscopic level, where layers of polymer side chains separated from layers of main chains, forming a sandwich type structure, as indicated by X-ray diffraction measurements.

In principle, poly(*p*-phenylene) would be expected to have exceptional mechanical properties due to the following: (1) molecular rotation is limited to rotation around a single axis; (2) the stiff nature of the backbone; (3) shape anisotropy of the polymer; and (4) the polymer readily formed ordered domains both in solution and in the melt. The introduction of side chains into the main chain successfully served to reduce the melting temperatures of these polymers, such that they could be readily processed from either solution or the molten phase. When considering that the polymer structure may be viewed as consisting of two microphases, layers of side chains separating layers of main chains, the orientation of the side chains is important for the overall mechanical properties. As mechanical properties are highly dependent on the symmetry of the molecular structure, chain packing density, and defects, the side chains may compromise the mechanical properties of these materials by the lack of orientation of the side chains within their microphase. The side chains would also be expected to limit the use of the materials at elevated temperatures, due to the relatively low temperature at which the side chains become liquid-like. The side chains appear to have a significant degree of local mobility, as shown by the low-temperature γ relaxation and the broad β relaxation. With the proper design of the side chains, i.e., the introduction of chemical units that have stronger intermolecular bonds, such as amide units, the side chains would (1) more effectively serve to bond the main chains together, (2) lead to an organization of the side chains having less defects, and (3) having a higher melting point, thus improving their high-temperature use. In this case, the melting temperature of the polymers was low enough such that, in future work, the side chains could be readily manipulated without obtaining intractable polymers.

Despite the large axial width of these materials, the high molecular weight polymers formed anisotropic melts that were shown by rheological measurements to be non-Newtonian shear thinning fluids. Of interest is the molecular weight dependence of the zero-shear viscosity for these materials. High molecular weight LC polymers showed a molecular weight dependence of the zero-shear rate viscosity typical of conventional polymer melts. By assuming the absence of entanglements as they are discussed for flexible polymers, flow would not be expected to be consistent with theory developed for the reptation of flexible chains. An activation energy for diffusion in the melt of 20.9 kJ/mol was calculated, which is a value typical of various linear polymers, suggesting that the mechanism of diffusion for these

polymers might be indicative of the mechanism of flow for isotropic melts. The motion of the chains in the melt may, however, not be governed by processes normally associated with flexible polymers involving the reptation model, but by corelated diffusion of bundles of chains or perhaps the reorganization of domains. Substituted poly(*p*-phenylene)s are ideal materials for the study of chain motion due to the lack of polar interactions and the definition of their shape. An investigation of the effect of side chain length on the flow properties of these materials might provide valuable insight into the general mechanism of polymer diffusion in the molten phase of main chain LC polymers.

Acknowledgment. Financial support from the Allied-Signal Corporation for this research is greatly appreciated.

References and Notes

(1) National Research Council, Committee on Liquid Crystal Polymers, Liquid Crystalline Polymers, Washington, D.C.; National Academy Press: Alexandria, VA, 1990; p xiv.
(2) Speight, J. G.; Kovacic, P.; Koch, F. W. *J. Macromol. Sci., Rev. Macromol. Chem.* **1971**, *C5*, 295.
(3) Kovacic, P.; Jones, M. B. *Chem. Rev.* **1987**, *87*, 357.
(4) Kovacic, P.; Kyriakis, A. *Tetrahedron Lett.* **1962**, 467.
(5) Kovacic, P.; Kyriakis, A. *J. Am. Chem. Soc.* **1963**, *85*, 454.
(6) Yamamoto, T.; Hayashi, Y.; Yamamoto, A. *Bull. Chem. Soc. Jpn.* **1978**, *51*, 2091.
(7) Berlin, A. A. *J. Polym. Sci.* **1961**, *55*, 621.
(8) Dacons, J. C. U.S. Patent 3450778, 1969.
(9) Ibuki, E.; Ozasa, S.; Murai, K. B. *Bull. Chem. Soc. Jpn.* **1975**, *48*, 1868.
(10) Stille, J. K.; Gilliams, Y. *Macromolecules* **1971**, *4*, 515.
(11) Taylor, S. K.; Bennett, S. G.; Khonry, I.; Kovacic, P. *J. Polym. Sci., Polym. Lett. Educ.* **1981**, *19*, 85.
(12) Marvel, C. S.; Hartzell, G. E. *J. Am. Chem. Soc.* **1959**, *41*, 448.
(13) Barrard, D. G. H.; Courtis, A.; Shirley, I. M.; Taylor, S. C. *J. Chem. Soc., Chem. Commun.* **1983**, 954.
(14) Barrard, D. G. H.; Courtis, A.; Shirley, I. M.; Taylor, S. C. *Macromolecules* **1988**, *21*, 294.
(15) Mckean, D. R.; Stille, J. K. *Macromolecules* **1987**, *20*, 1787.
(16) Miyaura, N.; Yanagi, T.; Suzuki, A. *Synth. Commun.* **1981**, *11* (7), 513.
(17) Kallitsis, J. K.; Rehahn, M.; Wegner, G. *Makromol. Chem.* **1992**, *193*, 1021.
(18) Rehahn, M.; Schlueter, A. D.; Wegner, G. *Polymer* **1989**, *30*, 1060.
(19) Rehahn, M.; Schlueter, A. D.; Wegner, G. *Makromol. Chem.* **1990**, *191*, 1991.
(20) Wallow, T. I.; Novak, B. M. *Polym. Prepr.* **1991**, *32* (3), 191.
(21) Wallow, T. I.; Novak, B. M. *Polym. Prepr.* **1993**, *34* (1), 1009.
(22) Wallow, T. I.; Novak, B. M. *Polym. Prepr.* **1992**, *33* (1), 1218.
(23) Wallow, T. I.; Novak, B. M. *J. Am. Chem. Soc.* **1991**, *113*, 7411.
(24) Flory, P. J.; Frost, R. S. *Macromolecules* **1978**, *11*, 1126.
(25) Flory, P. J.; Abe, A. *Macromolecules* **1978**, *11*, 1119.
(26) Witteler, H.; Lieser, G.; Wegner, G.; Schulze, M. *Makromol. Chem., Rapid Commun.* **1993**, *14*, 417.
(27) Conio, G.; Bianchi, E.; Ciferri, A.; Tealdi, A. *Macromolecules* **1981**, *14*, 1084.
(28) Aharoni, S. M. *Polym. Bull.* **1983**, *9*, 186.
(29) Duran, R.; Ballauff, M.; Wenzel, M.; Wegner, G. *Macromolecules* **1988**, *21*, 2897.
(30) Witteler, H. Ph.D. Dissertation, University of Mainz, Mainz, Germany, 1993.
(31) Earl, W. L.; Vanderhart, D. L. *Macromolecules* **1979**, *12*, 782.
(32) Hess, M.; Meierl, H.; Zech, B. *Spektroskopische Methoden in der Organischen Chemie*; Georg Thieme Verlag: Stuttgart, 1984.
(33) Fyfe, C. A.; Lyerla, J. R.; Volksen, W.; Yannoni, C. S. *Macromolecules* **1979**, *12*, 757.
(34) Whittaker, A. K.; Falk, U.; Spiess, H. W. *Makromol. Chem.* **1989**, *190*, 1603.
(35) Frech, B. C.; Adam, A.; Falk, U.; Boeffel, C.; Spiess, H. W. *New Polym. Mater.* **1990**, *2*, 267.
(36) Krevelen, D. W. V. *Properties of Polymers*; Elsevier Scientific Publ.: Amsterdam, 1976; p 345.
(37) Sabia, F. *J. Appl. Polym. Sci.* **1963**, *7*, 347.
(38) Marrucci, G. Rheology of Nematic Polymers. In *Liquid Crystallinity in Polymers*; Ciferri, A., Ed.; VCH Publishers: New York, 1991.
(39) Antonietti, M.; Foelsch, K. J.; Sillescu, H.; Pakula, T. *Macromolecules* **1989**, *22*, 2812.
(40) Roovers, J.; Graessley, W. W. *Macromolecules* **1981**, *14*, 766.
(41) Masuda, T.; Ohta, Y.; Onogi, S. *Macromolecules* **1986**, *19*, 2524.
(42) Winter, H. H.; Chambon, F. *J. Rheol.* **1986**, *30*, 367.

MA9464074